AIP | Applied Physics Letters

Combined plasmonic and dielectric rear reflectors for enhanced photocurrent in solar cells

A. Basch, F. J. Beck, T. Söderström, S. Varlamov, and K. R. Catchpole

Citation: Appl. Phys. Lett. **100**, 243903 (2012); doi: 10.1063/1.4729290
View online: http://dx.doi.org/10.1063/1.4729290
View Table of Contents: http://apl.aip.org/resource/1/APPLAB/v100/i24
Published by the American Institute of Physics.

Combined plasmonic and dielectric rear reflectors for enhanced photocurrent in solar cells

A. Basch,[1,2,a)] F. J. Beck,[3] T. Söderström,[4] S. Varlamov,[4] and K. R. Catchpole[1]
[1]*Centre for Sustainable Energy Systems, The Australian National University, Canberra ACT 0200, Australia*
[2]*Institute of Physics, University of Graz, Universitätsplatz 5, 8010 Graz, Austria*
[3]*ICFO, The Institute of Photonic Sciences, Barcelona, Spain*
[4]*ARC Centre of Excellence for Advanced Silicon Photovoltaics and Photonics, University of NSW, Sydney, NSW 2052, Australia*

(Received 5 April 2012; accepted 26 May 2012; published online 13 June 2012)

A doubling of the photocurrent due to light trapping is demonstrated by the combination of silver nanoparticles with a highly reflective back scatterer fabricated by *Snow Globe Coating* on the rear of a 2 μm polycrystalline silicon thin film solar cell. The binder free high refractive index titania particles can overcome light losses due to transmission. Modelling indicates that adding plasmonic nanoparticles to the back scatterer widens the angular distribution of scattered light such that over 80% of long wavelength light is scattered outside the Si/air loss cone and trapped in the cell, compared to 30% for the titania alone. © *2012 American Institute of Physics*. [http://dx.doi.org/10.1063/1.4729290]

To reduce the use of fossil fuels and to fulfill the increasing energy demand for the fast growing population of our planet, renewable energies need to be more efficient and cheaper. A way of reducing the silicon solar cell cost for today's technology is by using thinner layers and therefore less of the silicon material that accounts for about 50% of the photovoltaic module cost. However, due to weak absorption of infrared light in crystalline Si (c-Si), a significant fraction of solar energy is not converted into electricity in thin-film devices. Proper light management can potentially lead to ultra-efficient thin solar cells.[1] One method of achieving absorption enhancement in thin-film solar cells is through the excitation of localized surface plasmons in metal nanoparticles. These can be used as subwavelength scattering elements to couple a large fraction of incident light into trapped modes within a nearby semiconductor layer.[2–10]

The surface plasmon resonance (SPR) of metallic nanoparticles depends on the size, shape, and local dielectric environment of the particles. Recently, it has been shown that locating the nanoparticles on the rear of a solar cell is particularly effective in coupling long wavelength light into the cell.[11] In this configuration, the optimum in-coupling of light occurs when the resonance wavelength is in the vicinity of the band edge and the overlap of the near field of the resonance with the semiconductor is maximum.[12,13] This is achieved with hemispherical particles with heights of 50 nm or less and diameters in range of 100–160 nm that are located as close to the semiconductor as possible (with no or ultra-thin spacer layers).[13] It has been previously shown that the photocurrent enhancements achievable with plasmonic particles can be significantly increased by including a back reflector as this prevents scattered light being coupled out of the cell by the particles and lost. Ouyang *et al*. report a photocurrent enhancement of 29% when placing Ag particles on the rear of a 2 μm thick poly-Si thin film solar cell, increasing to 44% when combined with a detached diffuse back reflector.[14,15] For thinner glass superstrates, the enhancement could be further increased to 50%.[16]

High refractive index material coatings formed by coagulation of particles in solution have been reported to increase the photocurrent in a solar cell.[17] *Snow Globe Coating* is a method of forming highly effective diffuse back reflectors that is compatible with solar cell fabrication. To date, we have demonstrated short circuit current (J_{SC}) enhancements of 35% for 2 μm thick poly-Si thin film solar cells.[18] This simple and efficient process forms a binder-free coating of dielectric particles (rutile TiO_2, diameter: 1 μm) that provides very high reflection due to low absorption losses and high index contrast between the particles and the surrounding air.

In the present work, we combine *Snow Globe Coating* with plasmonic silver nanoparticles to achieve a J_{SC} enhancement of 100%, which is 73% of the value expected from an ideal Lambertian reflector. The structure combines a *Snow Globe Coating* layer, which provides very high reflectance but a relatively narrow angular scattering range (Figure 1(a)), with a plasmonic particle layer, which provides scattering into a broad angular range but which alone also leads to transmission losses (Figure 1(b)). The plasmonic particles ensure that over 80% of the scattered light near the band edge of silicon is directed outside the escape cone and hence trapped within the cell, while the *Snow Globe Coating* ensures that all light passes through the cell at least twice (Figure 1(c)).

Two micron thick poly-Si thin-film solar cells were formed on a glass substrate by electron beam evaporation followed by solid-phase crystallization. The cells consist of an emitter layer, an absorber layer, a back surface field and a silicon nitride antireflective coating on 3.3 mm thick borosilicate glass from Schott. The details of the design parameters and fabrication procedure are described elsewhere.[19,20]

The combined plasmonic–dielectric scattering layer was formed directly on the rear silicon surface of the cells by first fabricating the silver particle layer and then applying the *Snow Globe Coating*. To form the plasmonic particles, a

a)Author to whom correspondence should be addressed. Electronic mail: angelika@basch.at. Tel.: +436641773316.

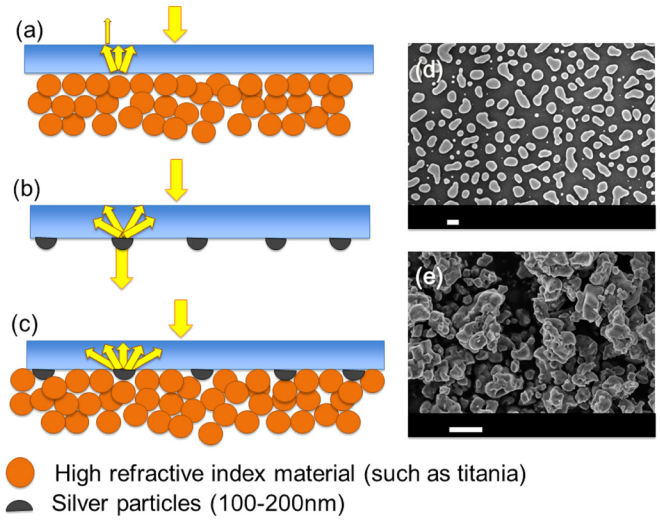

FIG. 1. Light trapping structures in solar cells using scattering by (a) *Snow Globe Coating*, (b) metallic nanoparticles (MNP) and (c) a combination of metal nanoparticles and a titantia coating, e.g., *Snow Globe Coating*. (d) Scanning electron micrographs of the silver particles (the scale bar is 100 nm) and (e) titania particles used in this study. The scale bar is 1 μm.

20 nm layer of silver was thermally evaporated ($p = 7 \cdot 10^{-6}$ mbar) onto the rear of a metallised pc-Si solar cell. Heating the silver films at 230 °C under nitrogen flow (120 L/h) for 50 min leads to the formation of particles directly on the solar cell surface, with a diameter of 100–200 nm as shown in the micrographs in Figure 1(d). The *Snow Globe Coating* was formed by placing the silver particle-coated pc-Si solar cell (silicon side up) into a 2000 mL beaker and pouring on a dispersion of titania particles (5 g dispersed by ultrasonication for 15 min in 1000 mL water). The particles of about 1 μm size settle by gravity. After 2 h, the cell is drawn out and dried. The titania particles used in this work were found to form a stable dispersion in water at *p*H 6–7.[18,21,22] The morphology of the titania particles forming *Snow Globe Coating* is shown in Figure 1(e). The coating process is based on self-assembly by settling particles dispersed in a liquid. Hence, the metal particles do not change the morphology of the titania layer.

To quantify the light trapping provided by the combined plasmonic and dielectric scattering layer, the photocurrent of the cells was measured with and without the scattering layer present. The spectral response of the solar cells was determined using a Xe lamp source, chopped at a frequency of 70 Hz, and filtered by a monochromator over a bandwith of 300–1400 nm. The photocurrent at each wavelength, with a bandwidth of 5 nm, was passed through a SR570 preamplifier, and displayed as a voltage across a SR830 DSP lock-in amplifier. The external quantum efficiency (EQE) was then calculated from the known illumination intensity as the fraction of incident photons that are converted to electrical current. During the measurement, the beam is split so that half falls on the test cell and half on an internal reference cell with a known spectral response. Prior to the measurement, the instrument was calibrated. To avoid variation in the measurement due to the non-uniformity of the semiconductor material, the measurements were performed on the same spot of the solar cell. Cells with combined plasmonic and dielectric scattering layers were mounted on the instrument

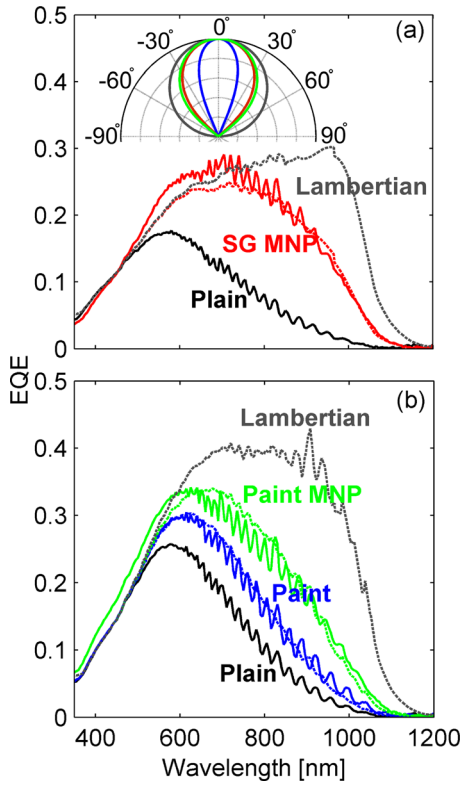

FIG. 2. (a) Experimental EQE data (solid lines) for the plain cell (Plain, black) and a cell with *Snow Globe Coating* and metal nanoparticles (SG MNP, red). The red dashed line shows the corresponding modeled EQE. The black dashed line shows the modeled EQE with a Lambertian rear reflector. (b) Experimental EQE data (solid lines) for the plain cell (Plain, black) and a cell with paint only (Paint, blue) and paint and metal nanoparticles (Paint MNP, green). The green and blue dashed lines show the corresponding modeled EQEs. The black dashed line shows the modeled EQE with a Lambertian rear reflector. The inset of (a) shows the angular distributions used in the modeling to fit the data.

and measured with light incident from the glass side. The *Snow Globe Coating* and silver particles were then removed physically by wiping with a wet cotton swab without moving or damaging the cell. The same spot was remeasured without the coating, for reference. For comparison, a similar procedure was followed using a sample with silver nanoparticles coated with commercial paint ("White Out" also known as "liquid paper" or "Tipp-ex"). For this sample, an additional measurement was taken for the cell coated in paint only, obtained by painting the same spot on the cell after the paint and silver particles were removed.

The red solid line in Figure 2(a) shows the EQE for the cell with *Snow Globe Coating* and silver particles (SG MNP), in comparison with the black solid line which shows the EQE for the reference cell (Plain). The EQE obtained for the silver particles coated by paint is shown in the green solid line of Figure 2(b) (Paint MNP), together with the paint only case shown in blue (Paint) and the black solid line of the plain cell for reference (Plain). It is clear from Figure 2(a) that the combined *Snow Globe Coating* and silver particles rear reflector substantially increases the photocurrent of the cell over a very large wavelength region, from 500 to 1100 nm. For comparison, the paint only case provides much smaller enhancements over this bandwidth, although this is increased by the inclusion of the silver nanoparticle layer.

In order to quantify the light trapping provided by the different rear coatings, we calculate the enhancement in the short circuit current (ΔJ_{SC}) relative to the planar reference case (Plain in Figure 2). The J_{SC} was calculated by

$$J_{SC} = q\int EQE(\lambda)S(\lambda)d\lambda,$$

where q is the electron charge, S is the standard spectral photon density of sunlight at the earth's surface (Air Mass 1.5). The combined *Snow Globe Coating* and silver particles reflector (SG MNP in Figure 2(a)) increases the J_{SC} by 100% over the spectrum measured. For comparison, the paint only case (Paint in Figure 2(b)) provides a ΔJ_{SC} of 22%, increasing to 66% with the inclusion of a silver nanoparticle layer (Paint MNP in Figure 2(b)). The results of the J_{SC} calculations are given in full in Table I. As noted in the introduction, for the same type of solar cells, previous work with metal nanoparticles only has given an enhancement of 29% (increasing to 44% with the addition of a back reflector),[14] while previous work with *Snow Globe Coating* only has given an enhancement of 35%.[18]

A simple optical model was used to characterize the enhanced light trapping effect by combining plasmonic scatterers with *Snow Globe Coating* or paint. The transfer matrix method is employed to calculate the transmission and reflection at each interface of a multilayered structure. To model rear located diffuse scatterers, the method of Götzberger was used,[15,16] with reflectance and the angular distribution of scattered light as input.[13,23,24] Light incident at the rear interface of the Si active layer, given by the reflectance, is scattered in a given angular distribution. Light propagating inside the loss cone is lost at the front surface while light propagating outside the loss cone is totally internally reflected and re-scattered at the back surface. The Götzberger formalism keeps track of the absorption due to the increase in the path length of the scattered light inside the absorbing layer. The scattering distribution of the diffuse rear reflectors was modelled using a "narrowed Lambertian" approach by applying the method of Cotter.[25] This method takes into account the refraction of the scattered light originating in a medium with effective refractive index n_{eff}, as it enters the Si layer with n_{Si}. The angular distribution is then given by: $I_\theta = \cos[\text{asin}((n_{Si}/n_{eff})\sin\theta)]$. This allows the angular distribution to be modified in the model in a controlled way. The fraction of the scattered light that is trapped inside the silicon layer, F_{LT}, is then calculated by integrating over angles outside the Si/Air loss cone and normalizing to the total scattered light.

TABLE I. Enhancements of short circuit currents (ΔJ_{SC}) in combined plasmonic (MNP) and dielectric scattering obtained by *Snow Globe Coating* (SG) and paint, noting that the J_{SC} values have been rounded to one decimal place.

	J_{SC} (mA/cm^2)	ΔJ_{SC}
Plain cell	4.0	-
SG + MNP	8.0	100%
Plain cell	5.7	-
Painted cell	7.2	28%
Paint + MNP	9.4	66%

For the paint and the *Snow Globe Coating*, n_{eff} has a physical meaning, and the resulting angular distribution is due to refraction of the scattered light at the Si interface. For the *Snow Globe Coating* and paint only scattering surfaces, the n_{eff} approach is a good approximation to the physical picture as the scattering layer is roughly Lambertian and the narrowing of the angular distribution is due to refraction at the Si interface.[25] Here the n_{eff} can be approximated as the effective refractive index of the scattering medium. For the *Snow Globe Coating* and paint, n_{eff} also serves as a number that can characterize how effective the scattering is, compared to a Lambertian distribution (which has $n_{eff} = n_{Si}$).

For the cases with the metal nanoparticles, n_{eff} does not have the physical meaning of an effective index of the metal nanoparticle layer, but it is still a number that can be used to characterize the scattering. The metal nanoparticles are directly fabricated on the Si surface and have been shown to have a relatively wide angular distribution in the Si.[13] Here n_{eff} is increased to widen the angular distribution in the model in a controlled way, to gain insight into the effect of the inclusion of the nanoparticles in the scattering layer.

The cells are modeled as a layered stack consisting of a 2 μm thick pc-Si layer coated with a 100 nm silicon nitride film on a semi-infinite glass superstrate. As in the experimental case, the light was incident from the glass superstrate. The n, k values for c-Si were taken from data from Keevers and Green,[26] with k corrected for the higher absorption in pc-Si between 400 and 700 nm with data from He and Sproul.[27] The n value of the silicon nitride was taken as 2.0, which agrees well with experimentally determined values. The finite thickness of the glass was taken into account by assuming that light that is within the escape cone for Si/glass but outside the escape cone for Si/air is returned to the silicon. Using this approach, the absorption in the silicon could be calculated for different angular distributions (by varying n_{eff}) and reflectance of the scattering layer.

A wavelength dependent "modeled internal quantum efficiency (IQE)" was defined by dividing the experimental EQE spectra for the reference (Plain) cell by the calculated absorption of the same cell (smoothed to extract the interference fringes). As the EQE spectra for reference cells given in Figs. 2(a) and 2(b) are different, separate modeled IQE are calculated for each. The calculated absorption in a poly-Si cell with the different diffuse reflectors was multiplied by this modeled IQE to obtain a modeled EQE that could be directly compared to the experimental data. The angular distribution (by varying n_{eff}) and the reflectance, R, used in the model were chosen empirically by fitting the modeled data to the experimental EQE by eye. In this way, we study the differences between the light trapping efficiencies of the *Snow Globe Coating* and the paint with and without Ag nanoparticles present, in terms of the scattering angular distribution and the reflectance of the layer.

The dashed red line in Figure 2(a) shows the modeled EQE spectra, compared to the experimentally measured data (solid red line) for the combined *Snow Globe Coating* and metal nanoparticles. Figure 2(b) shows the corresponding results for the paint coating, with and without metal nanoparticles. The modeled EQE spectra agree well with the experimental data in all cases. The resulting J_{SC} enhancements

(ΔJ_{SC}) are summarized in Table II. It can be seen that the model also gives very good agreement with the experimental J_{SC} enhancements.

Table II lists the inputs, n_{eff} and R, used to obtain the modeled results, and the inset in Figure 2(a) shows the angular distribution of the light scattered by coatings with different values of n_{eff}. The case of paint only has a relatively narrow angular distribution corresponding to 30% of the scattered light being trapped at long wavelengths, given by $n_{eff} = 1.4$, and a reflectance, R, of 85%, in agreement with previous results.[18] It has been previously found that *Snow Globe Coating* also leads to relatively narrow angular distribution (value of $n_{eff} = 1.4$), but with a much higher reflectance of approximately 100%.[18] We can see from Table II that combining the *Snow Globe Coating* with metal nanoparticles maintains the very high reflectance of the *Snow Globe Coating*, but substantially widens the scattering distribution, increasing the n_{eff} to 2.6. This increases the fraction of the scattered light that is trapped at long wavelengths to 80%. For the case of paint, including metal nanoparticles also substantially widens the angular distribution such that 83% of the scattered is light trapped for $\lambda > 1000$ nm, (increasing n_{eff} to 2.8). However, in this case, the reflectance is also somewhat increased, from 85% to 90%.

From these results, we can conclude that the main effect of the metal particles when a back reflector is present is to broaden the angular distribution of the scattered light, i.e., increase n_{eff}. This results in a much larger fraction of the light being scattered outside the escape cone of the silicon and hence eventually being absorbed and contributing to the photocurrent. Where the reflectance is relatively low, as in the case of paint, the metal particles can also act to increase the reflectance. This is because silver particles with the dimensions used here have an albedo (i.e., ratio of scattering to extinction) of close to 100%.[3] Thus, if light interacts with the particles rather than the paint, it is more likely to be scattered rather than lost, i.e., the metal nanoparticles can reduce the fraction of light absorbed in the paint.

Also shown in Figures 2(a) and 2(b) are the EQE spectra that would be expected from the cells with an ideal Lambertian back reflector ($R = 100\%$, $n_{eff} = n_{Si}$). As the cells shown in Figs. 2(a) and 2(b) have different reference spectra and hence different modeled IQEs, the enhancements due to light trapping cannot be directly compared. For this reason, we compare the enhancements as fractions of the ideal Lambertian case. The J_{SC} enhancement achieved with the *Snow Globe Coating* combined with plasmonic particles is 100%. Using the modeled IQE for this cell, the enhancement achievable with a Lambertian reflector ($R = 100\%$, $n_{eff} = n_{Si}$) would be 138%, i.e., the experimental enhancement is 73% of that expected from a Lambertian reflector. In Ref. 18, we report that *Snow Globe Coating* alone (without MNPs) increases the Jsc by around 38% of the Lambertian case. For the combination of paint and plasmonic particles, the enhancement is 51% of the Lambertian value, while for paint only the enhancement is 22%. The details of these results are given in Table II. The higher enhancement for the plasmonic particles combined with *Snow Globe Coating*, compared to the particles combined with paint, is due to the higher reflectance of the *Snow Globe Coating*.

We can also compare these results with modeled results using inputs derived from a single disk shaped silver nanoparticle obtained from finite-difference time-domain (FDTD) modeling. It has been previously estimated using FDTD that a silver disk directly on a silicon surface leads to a scattering efficiency (albedo) of 90%.[13] The angular scattering distribution associated with this particle was also calculated. Using these parameters as inputs to the present model, and using the modeled IQE, we calculate that a photocurrent enhancement of 105% would be expected (Table II).

For the *Snow Globe Coating*, the model does underestimate the enhancement in the EQE at wavelengths between 500 and 700 nm. The underestimation in the model remains even when an ideal Lambertian type reflector is used, suggesting that it is not due to an optical effect. This effect has been seen previously with titania back reflectors.[18] This anomalously high EQE enhancement at short wavelengths could be due to an increase in the IQE of the cell, due to a redistribution of generated charge carriers to regions of the cell where they have a higher probability of collection.

There are a few key factors, for both the silver particles and the *Snow Globe Coating*, that lead to the high photocurrent enhancement observed here. For the silver particles, the main factors are their size and location.[12] The size of the silver nanoparticles is in the range of 100–200 nm, which leads to high scattering efficiency and low parasitic absorption. The particles are located directly on the silicon and have a high contact area with the interface (roughly hemispherical or disk shaped rather than spherical), leading to effective coupling into the silicon. Because the particles are directly on the silicon, the surface plasmon resonance is also redshifted into the region of the spectrum where silicon absorbs weakly, making light trapping more effective. In addition, the scattering cross-section is enhanced for particles directly on silicon.[28]

TABLE II. Integrated J_{SC} enhancements (ΔJ_{SC}) for measured and modeled cells (between 350 and 1200 nm). Also shown are the inputs n_{eff}, R used to calculate the modelled data in each case. The fraction of light scattered outside the loss cone and trapped, F_{LT}, is shown for each n_{eff}. The ΔJ_{SC} for the different coatings are given as the fraction of the enhancement calculated for an ideal Lambertian reflector.

Coating	n_{eff}	F_{LT} (%)	R	$\Delta J_{SC\ MODEL}$	$\Delta J_{SC\ EXP}$
SG + MNP	2.6	80	100	89	100
Lambertian	nSi	92	100	138	–
% of Lambertian Enh: SG + MNP				**65**	**73**
Paint	1.4	33	85	29	28
Paint + MNP	2.8	83	90	60	66
Lambertian	nSi	92	100	130	–
% of Lambertian Enh: Paint				**22**	**22**
% of Lambertian Enh: Paint + MNP				**46**	**51**
Ideal MNP[a]	–	91	–	105	–
Lambertian	nSi	92	100	138	–
% of Lambertian Enh: ideal MNP				**76**	**–**

[a]Single disk shaped MNP on the rear of a Glass|SiN|Si|Air substrate. The angular distrubution is given by the modelled scattering distrubution for a single particle on an infinite Si substrate and R is given by the calculated scattering efficiency of an ideal particle (η_{scat}), as described in Ref. 13. This assumes that $F_{subs} = 1$ and that parasitic absorption is the only loss mechanism.

For the *Snow Globe Coating* titania layer, there are also several important parameters. The titania particles have a high refractive index and are similar in size to the wavelength of light, so they scatter light strongly. The coating does not contain a binder, which increases scattering further due to a higher refractive index contrast between the titania particles and the surrounding air. In addition, the layer is sufficiently thick that there is no transmission through the layer. In order to achieve low losses and effective scattering of the light, all of these factors associated with the metal particles and the titania layer must be considered.

We have demonstrated 100% increase in photocurrent of thin film silicon solar cells using a back reflector structure that combines plasmonic particles to scatter light at high angles, and a titania coating to ensure that no light escapes out the rear of the cell. For the titania coating, the colloidal deposition technique *Snow Globe Coating* gives higher enhancements than paint when combined with silver particles because of its very high reflectance. The approach presented here demonstrates how the advantages of plasmonic and dielectric structures can be used selectively to maximise the performance of a device.

This project was funded by the Austrian Science Fund (FWF): J-2979, the Australian Research Council and the Australian Solar Institute. We thank the Centre for Advanced Microscopy and the Australian Microscopy & Microanalysis Research Facility for access to ZEISS ultra plus. We would like to thank Er-Chien Wang and John W. White from the Australian National University for their help.

[1]A. Polman and H. A. Atwater, Nature Mater. **11**, 174 (2012).
[2]H. A. Atwater and A. Polman, Nature Mater. **9**, 205 (2010).
[3]H. R. Stuart and D. G. Hall, Appl. Phys. Lett. **73**, 3815 (1998).
[4]K. R. Catchpole, S. Mokkapati, F. J. Beck, E. C. Wang, A. McKinley, A. Basch, and J. Lee, MRS Bull. **36**, 461 (2011).
[5]D. Derkacs, S. H. Lim, P. Matheu, W. Mar, and E. T. Yu, Appl. Phys. Lett. **89**, 093103 (2006).
[6]R. A. Pala, J. White, E. Barnard, J. Liu, and M. L. Brongersma, Adv. Mater. **21**, 3504 (2009).
[7]C. Hägglund, M. Zäch, G. Petersson, and B. Kasemo, Appl. Phys. Lett. **92**, 053110 (2008).
[8]T. L. Temple, G. D. K. Mahanama, H. S. Reehal, and D. Bagnall, Sol. Eng. Mater. Sol. Cells **93**, 1978 (2009).
[9]A. J. Morfa, K. L. Rowlen, T. H. Reilly III, M. J. Romero, and J. v. d. Lagemaatb, Appl. Phys. Lett. **92**, 013504 (2008).
[10]G. Qilin, J. Phys. D: Appl. Phys. **43**, 465101 (2010).
[11]F. J. Beck, S. Mokkapati, A.Polman, and K. R. Catchpole, Appl. Phys. Lett. **96**, 033113 (2010).
[12]K. R. Catchpole and A. Polman, Appl. Phys. Lett. **93**, 191113 (2008).
[13]F. Beck, S. Mokkapati, and K. R. Catchpole, Opt. Express **19**, 25230 (2011).
[14]Z. Ouyang, S. Pillai, F. Beck, O. Kunz, S. Varlamov, K. R. Catchpole, P. Campbell, and M. A. Green, Appl. Phys. Lett. **96**, 261109 (2010).
[15]Z. Ouyang, X. Zhao, S. Varlamov, Y. Tao, J. Wong, and S. Pillai, Prog. Photovoltaics **19**, 917 (2011).
[16]S. Varlamov, paper presented at the Photonics Global Conference, Singapore, 2010.
[17]B. G. Lee, P. Stradins, D. L. Young, K. Alberi, T.-K. Chuang, J. G. Couillard, and H. M. Branz, Appl. Phys. Lett. **99**, 064101 (2011).
[18]A. Basch, F. J. Beck, T. Söderstrom, S. Varlamov, and K. R. Catchpole, "Enhanced light trapping in solar cells using snow globe coating," Prog. Photovoltaics (in press).
[19]O. Kunz, Z. Ouyang, S. Varlamov, and A. G. Aberle, Prog. Photovoltaics **17**, 567 (2009).
[20]T. Söderstrom, Q. Wang, K. Omaki, O. Kunz, D. Ong, and S. Varlamov, Phys. Status Solidi (RRL) **5**, 181 (2011).
[21]A. Basch, in *Coagulation: Kinetics, Structure Formation and Disorders*, edited by A. M. Taloyan and D. S. Bankiewicz (Nova Science Publishers, 2012).
[22]A. Basch, S. Strnad, and V. Ribitsch, Colloids Surf., A **333**, 163 (2009).
[23]A. Götzberger, in *Proc. 15th Photovoltaic Specialist Conference* (1981).
[24]M. A. Green, Prog. Photovoltaics **10**, 235 (2002).
[25]J. E. Cotter, J. Appl. Phys. **84**, 618 (1998).
[26]M. J. Keevers and M. A. Green, Appl. Phys. Lett. **66**, 174 (1995).
[27]S. He and A. B. Sproul, Thin Solid Films **519**, 351 (2010).
[28]F. J. Beck, E. Verhagen, S. Mokkapati, A. Polman, and K. R. Catchpole, Opt. Express **19**, A146 (2011).